Investigation of the laminar burning velocity of premixed H_2-air flames highly diluted with exhaust gas using the heat-flux burner method

M. Schneider[1]*, M. Bauer[1], P. Habisreuther[1], C. Weis[1], B. Stelzner[1], D. Trimis[1]

[1]Engler-Bunte-Institute, Division of Combustion Technology, Karlsruhe Institute of Technology, Karlsruhe, Germany

Abstract

The laminar burning velocities of H_2-air and H_2-air flames highly diluted with recirculated exhaust gas were calculated using the freely propagating flame algorithm of ANSYS Chemkin Pro. In order to calculate the effect of recirculating exhaust gas, a simplified equilibrium composition that is experimentally accessible was generated and mixed with inlet streams varying air factor, preheat temperature and heat loss of exhaust gases. Besides, three different chemical mechanisms have been applied and compared.

The results show that with increasing exhaust gas recirculation (EGR) the overall flame speed is decreasing and the flame speed maximum is shifted towards higher air factors. The comparison of the chemical mechanisms showed that the more recent Konnov-2019 and NUIG Mech1.1 show similar trends, whereas the older Kéromnès predicts higher flame speeds. Above the heat loss from the exhaust gas was investigated and showed that with less heat loss timescales of chemical kinetics become more pronounced resulting in higher flame speeds at an air factor of $\lambda = 1.0$.

Introduction

With the advancing decarbonization of the energy market, it can be assumed that hydrogen will be available on a large scale in the near future playing an important role in end-use applications [1]. In addition to the use of synthetic hydrocarbons produced from "green" hydrogen, the combustion of carbon-free chemical energy sources is an attractive option for avoiding CO_2 emissions. In this context hydrogen produced by water electrolysis for the storage of excess renewable power can be used as a primary energy carrier [2]. However, due to its combustion characteristics, conventional burner systems are often not suitable for operation with pure hydrogen. Accordingly, there is a need for new developments which are designed for operation with pure hydrogen where process heat is needed. In present studies the main focus is on hydrogen enriched methane-flames [3,4] and is slowly shifting towards hydrogen only combustion.

The combustion properties of hydrogen are very different from those of conventional hydrocarbons. The high burning velocity of hydrogen-air flames of around 320 cm/s at an air factor of 0.6 must be mentioned in this context [5]. In addition, high diffusion rates in the flame region lead to very short reaction zones and to thermo-diffusive flame instabilities [6].

These reasons lead to the fact that hydrogen is not burned premixed in current technical systems due to operational safety. On the other side, non-premixed combustion leads to locally high peak temperatures and thus promotes the formation of nitrogen oxide in the exhaust gas, which also severely restricts the operating ranges and controllability of technical applications. In a premixed system, there is also the risk of flashback [7,8], which strongly increases when pure hydrogen is used as fuel due to the increased diffusivity and flame speed in combination with a reduced quenching distance. Due to a smaller quenching distance, hydrogen-air flames propagate closer along walls than other fuels before extinguishing. In automotive engines this strongly increases the tendency to backfire because the hydrogen-air mixture passes closer to the intake valve than hydrocarbon flames [9]. Hydrogen engines are also characterized by higher NO_x concentrations compared to hydrocarbon fuels [10].

In order to handle these issues that are related to hydrogen-air combustion, dilution with steam or nitrogen is often used [11]. The experimental and numerical results of Lu et al. [12] show that the NO emission at steam dilution is about 20-50 % of the emission present at N_2 dilution at the same equivalence ratio and dilution ratio due to the direct chemical and third-body effects of steam reducing the formation of NO mainly in the NNH pathway.

Another option to better control premixed hydrogen combustion is to recirculate exhaust gas. Right now the exhaust gas recirculation (EGR) concept is mainly used in SI engines [13,14] or turbines [15]. One of the key technologies for pure hydrogen combustion due to its ability to reduce NO_x emissions [16,17]. EGR acts as an additional diluent in the unburned gas mixture, lowering peak combustion gas temperatures and NO_x formation rates [18], provided that an appropriate amount of heat is removed from the exhaust gases. Moreover, mmeasurements on a spherically expanding flame at constant pressure performed by Duva et al. [19] showed that the flame speed and the adiabatic flame temperature decrease almost linearly with increasing degree of dilution through EGR. This effect could also by shown by Wang et al. [20].

Numerical Approach

The numerical calculations carried out in the current study employ the CKReactorFreelyPropagatingFlame program of the ANSYS Chemkin Pro 21 package [21]. The program is a further development of the PREMIX code originally developed by Kee et al. [22] that solves

* Corresponding author: Michael.schneider2@kit.edu

the 1D, steady state balance equations of species and energy that describe the flame dynamics in a laminar premixed planar flame using implicit finite difference methods. The solution algorithm uses a coarse-to-fine grid refinement in order to provide optimal mesh placement. Typically, calculations start with a coarse grid of about 10-30 points and are assumed to be grid independent at a number of 300-600 points, depending on the complexity of the used chemical scheme. Grid independence is assessed using normalized criteria with respect to maximal changes in the values and gradients of species between adjacent points (0.05 and 0.07). The freely propagating flame algorithm is employed to determine the characteristic flame speed of the gas mixture at the specified pressure and inlet temperature. It automatically adjusts the velocity at the inlet of the problem to maintain the fluid velocity constant at a point in the flame with a selected temperature.

The simulations were conducted using the Konnov mechanism for hydrogen combustion from 2019 [23], the mechanism from National University of Ireland Galway called NUIG Mech1.1 from 2020 [24] and the Kéromnès mechanism from 2013 [25]. The review of Olm et al [26] comparing the performance of several hydrogen combustion mechanisms that were present before 2014 showed that the Kéromnès mechanism performed best calculating flame velocities. This is the reason why this mechanism was chosen amongst the other two more recent mechanisms.

The aim of the numerical calculations was to determine the dependence of the laminar flame velocity under the influence of recirculating exhaust gases. The purpose of exhaust gas recirculation (EGR) is manifold, as it offers the possibility to manipulate extensive thermodynamic quantities by additional fluxes, such as enthalpy, which changes its value only by a flux across the system boundary (e.g., by heat removal). Without heat flow across the system boundary, the total enthalpy (sum of sensible enthalpy and formation enthalpy) remains constant. Furthermore, the final state (equilibrium) remains the same regardless of mixing within the system. The reaction path to reach the equilibrium state also usually remains similar.

When exhaust gas is recirculated and heat is removed from this fluid stream, its total energy decreases. Thus, mixing such a gas mixture with fresh fuel results in a composition with lower enthalpy, so that the maximum possible temperature after combustion is also reduced. The amount of removable heat from exhaust gases depends on the technical realization.

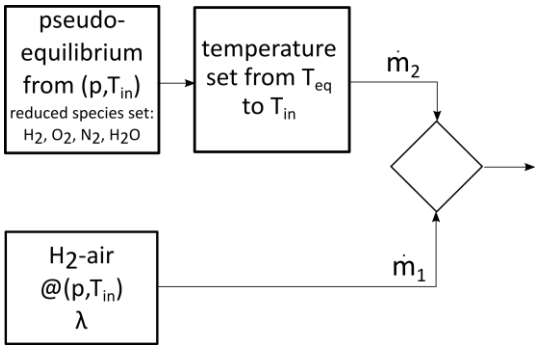

Figure 1: Sketch illustrating the generation of inlet conditions for laminar flame calculations with maximum heat loss

The first calculation series investigates the pure influence of recirculation rate using as a maximum estimation that the temperature of the recirculated flow is reduced to the preheating temperature T_{in}. Figure 1 illustrates for this assumption the generation of inlet conditions for the laminar flame calculations with maximum heat loss. In a first stream $\dot{m}_1$ fresh H_2-air mixture is used with air factor λ, pressure p and the inlet temperature T_{in}. The composition of a second stream is calculated using the equilibrium code of ANSYS Chemkin Pro for the same mixture, but restricting the possible species-set to the components H_2, O_2, N_2 and H_2O. The resulting mixture composition and temperature T_{eq} of this pseudo-equilibrium is then artificially set to the inlet temperature T_{in} of the first mixture. The inlet conditions for the 1D hydrogen flame calculation is then calculated by a massflow weighted mixture of the two described streams.

Equation *(1)* shows the definition of the exhaust gas recirculation rate EGR as the fraction of mass flows $\dot{m}_2$ and $\dot{m}_1$:

$$EGR = \frac{\dot{m}_2}{\dot{m}_1} \qquad (1)$$

In order to additionally look at the influence of the amount of heat that is removed from the recirculated flow, a specified heat-loss needs to be applied to the recirculated (equilibrium) gas. This can be done by additional processing of the pseudo equilibrium results with the perfectly stirred reactor model of ANSYS Chemkin Pro. The residence time is chosen to be sufficiently large for the system to adapt to this heat loss (~ 1-2 sec), regardless of technical realizability at this stage.

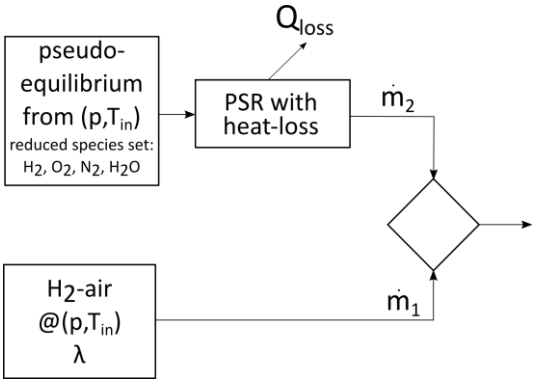

Figure 2: Sketch illustrating the generation of inlet conditions for laminar flame calculations with specified heat-loss

In order to assess the heat-loss specified for the recirculated mixture a normalized quantity H^* was used. This relative enthalpy has been defined relating the heat loss Q_{loss} that is applied to the perfectly stirred reactor to the difference of mixture enthalpies of equilibrium state and of a mixture with the equilibrium composition H_{eq} and fresh gas temperature H^*_{fg}.

$$H^* = \frac{Q_{loss}}{H_{eq} - H^*_{fg}} \qquad (2)$$

As a consequence, the enthalpy of the stream from the outlet of the perfectly stirred reactor H_{PSR} is the difference between H_{eq} and Q_{loss}:

$$H_{PSR} = H_{eq} - Q_{loss} \qquad (3)$$

It is clear that H^* =0 denotes no heat-loss and H^* =1 approximates the maximum heat-loss with recirculated flow temperature approximating the one of fresh gas, similar to procedure shown in Figure 1.

Results and Discussion

Figure 4 shows the laminar flame speed of hydrogen-air flames in cm/s as a function of air factor λ for the inlet temperature of 300 K on the left-hand side and for the inlet temperature of 673 K on the right-hand side. The results were obtained using the Konnov mechanism from 2019 [23] and show the laminar flame speed over air factor between $0.3 \leq \lambda \leq 3.0$ varying the EGR rate from 0 (in black) to 1.0 (in red) in 0.2 steps. Additionally, the fresh gas inlet temperatures was varied (300 K, 373 K, 473 K, 573 K and 673 K). The graphs show exemplarily the inlet temperatures of 300 K and 673 K.

The maximum in flame speed for both graphs are with an EGR ratio of 0.0 at approximately 320 cm/s for an air factor of λ = 0.6 on the left-hand graph and at around 1140 cm/s for an air factor of λ =0.55 on the right-hand graph. After reaching the maximum flame speed the flame speed is decreasing with increasing air factor. For both inlet temperatures is obtained that with increasing EGR rate the flame speed is decreasing and the flame speed maximum is shifted towards higher air factors. For an EGR rate of 1.0 and an inlet temperature of 300 K the maximum flame speed of approximately 60 cm/s is reached at an air factor of λ = 0.75. For an inlet temperature of 673 K and an EGR rate of 1.0 the maximum flame speed of approximately 480 cm/s is reached at an air factor λ = 0.65. The shift towards higher air factors with increasing EGR rate is more pronounced for lower inlet temperatures and for higher

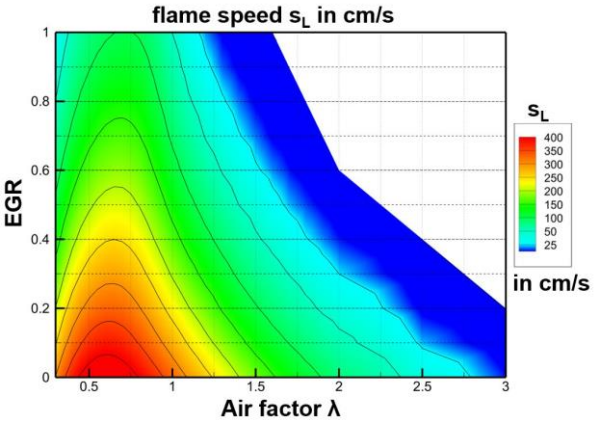

Figure 3: Flame speed of H_2-air mixtures as a function of the air factor and recirculation ratio (EGR) at p_0 = 1 bar and T_{in} = 373 K

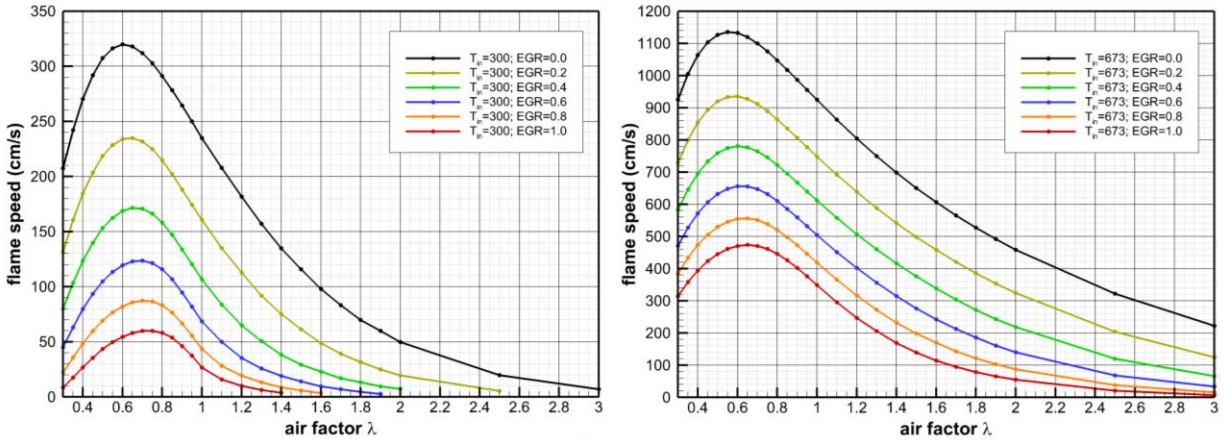

Figure 4: Flame speed of hydrogen-air flames in cm/s as function of the air factor λ for inlet temperature of 300 K (left) and 673 K (right) for different EGR rates (0, 0.2, 0.4, 0.6, 0.8, 1.0) (p_0 = 1 bar)

inlet temperatures the maximum flame speed is shifted slightly towards lower air factors.

Figure 3 plots the laminar flame speed as iso-color plot varying the air factor and EGR as a colored gradation. High flame speeds are shown in red color, and lower flame speeds are depicted in blue color. The turquoise region between 25 cm/s and 50 cm/s represents the operating range, which includes the usual methane-air combustion range of 37 cm/s (stoichiometric and at standard conditions) [27]. It can be observed, that the turquoise region spans from lower right to the upper left, i.e. at higher EGR this domain is located at lower air factors. E.g. at an EGR of 0, the area is at an air factor λ of about 2.5, while at an EGR of 1.0, the area shifts to an air factor λ of 1.2.

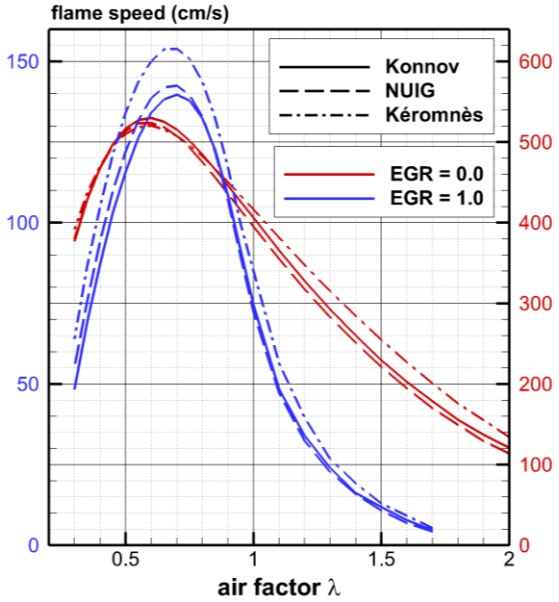

Figure 5: Flame speed of H_2-air mixtures as a function of the air factor for three different kinetic mechanisms (Konnov, NUIG, Kéromnès) with EGR 0.0 and 1.0 with p_0 = 1 bar and T_{in} = 423 K

In order to assess the flame speed results at the conditions imposed by EGR three different chemical schemes have been applied. Figure 5 shows the flame speed as a function of the air factor for three different kinetic mechanisms at a pressure of p_0 = 1 bar and an inlet temperature of fresh gas of T_{in} = 423 K. The results with EGR 0.0 are shown in red and the results with EGR 1.0 are shown in blue. The solid lines are computed with the kinetic mechanism of Konnov [23], the dashed lines with the NUIG Mech1.1 [24] and the dashed-dotted lines with the Kéromnès mechanism [25]. The overall trend in flame speed is for all the mechanisms the same and the maximum flame speed is reached at the same air factors for both EGR rates. It can be observed that the more recent mechanisms NUIG Mech1.1 and Konnov-2019 show very similar values in flame speed with and without EGR, whereas the Kéromnès mechanism predicts slightly higher flame speeds which is more pronounced in the case with EGR. In this case the Kéromnès mechanism predicts an approximately 10 % higher flame speed in comparison to the Konnov-2019 mechanism over a wide range of air factors. Only at high air factors and low flame speeds the graphs show the same trend. In the scenario without EGR the flame speed of all mechanisms show similar values for air factors below 1. For air factors λ > 1.0 the Kéromnès mechanism predicts higher flame speeds.

Figure 6 shows the laminar flame speed of hydrogen-air flames in cm/s as function of air factor λ for the inlet temperature 473 K and heat loss H* = 0.7 on the left-hand side and heat loss H* = 0.8 on the right-hand side. H* is defined using equation (2). The result for EGR 0.0 is the same in both graphs and reaches its maximum in flame speed at air factor λ = 0.6 with approximately 630 cm/s. In the left-hand side case less heat is removed from the exhaust gas (H* = 0.7) in comparison to the right-hand side case (H* = 0.8). Therefore, the recirculated exhaust gas has a higher temperature before it is admixed to the fresh gas in the H* = 0.7 case.

Most noticeable in Figure 6 is an unexpected local maximum that is visible at air factor 1.0 for increased EGR and is more pronounced for the lower heat-loss case H*=0.7. This can be explained by the fact, that

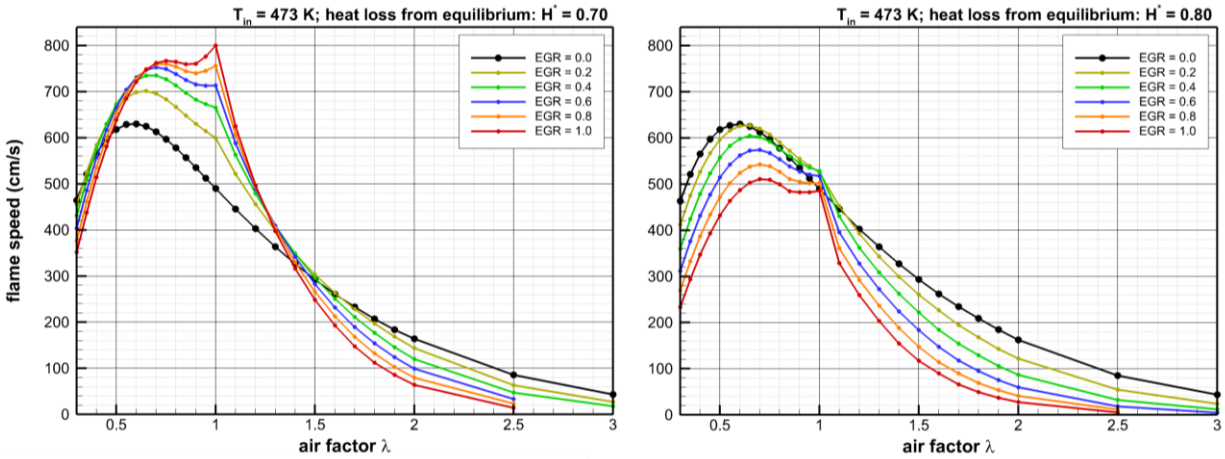

Figure 6: Flame speed of hydrogen-air flames in cm/s as function of the air factor λ for inlet temperature of 473 K for different EGR rates (0, 0.2, 0.4, 0.6, 0.8, 1.0) for H = 0.7 heat loss (left) and H* = 0.8 heat loss (right). (p = 1 bar)*

corresponding to a decrease of H* an increase of temperature at the inlet of the laminar flame is a result of recirculation. Of cause this increase is more pronounced when less heat is removed from the recirculating gases, i.e. at lower H*. If H* is decreased to even lower values than 0.7, a domain of air factor around the stoichiometric value can be observed, where autoignition prevents a solution of the freely propagating flame problem. As auto-ignition is ruled by the timescales of chemical kinetics, the phenomenon is most pronounced at stoichiometric air factor. Decreasing H* down to 0.7 and below thus leads to a transition to the conditions, where auto ignition occurs, showing increased flame speed.

In the right-hand side case, the maximum in flame speed shifts towards higher air factors and to lower flame speed values for increasing EGR. It can be obtained that a local maximum is reached at an air factor of $\lambda = 1.0$ which is only present with EGR and more pronounced with increasing EGR rate. Around the air factor of $\lambda = 1.0$ the values of flame speed for EGR 0.2 – 0.8 also exceed the value of EGR 0.0 in a small range of air factor.

In the left-hand side case the effect described before is even more present. The maximum in flame speed is also shifted towards higher air factors with increasing EGR. However, in this case the maximum in flame speed is shifted towards higher values with increasing EGR. Again, a local maximum in flame speed is reached at an air factor of $\lambda = 1.0$ which is also a global maximum for an EGR rate of 1.0. In the range of $0.4 \leq \lambda \leq 1.4$ the values in flame speed for any EGR exceed the case of EGR 0.0. After reaching the turning point at an air factor of $\lambda \approx 1.4$ a higher EGR rate leads to lower flame speeds for $\lambda > 1.4$.

Conclusions

The current investigation focuses on the influence of exhaust gas recirculation (EGR) on the flame speed of hydrogen-air mixtures. In this case, an extensive series of calculations have been conducted varying the inlet temperature, the air factor and the EGR rate using three different kinetic mechanisms. Besides an additional series of calculation have been performed analyzing the influence of the EGR with different amount of heat-loss applied to the recirculated exhaust gas before it is admixed to the fresh gas.

An analysis of the results with reference to the procedure shown in Figure 1 showed that with increasing EGR the overall flame speed is decreasing and the flame speed maximum is shifted towards higher air factors. This effect is more pronounced for lower inlet temperatures. An increased inlet temperature leads to an overall higher flame velocity.

When an operation range is aimed for that reaches equal flame speeds in comparison to methane-air combustion EGR makes it possible to reduce the air factors from 2.5 without EGR to $\lambda = 1.2$ with an EGR of 1.0.

Furthermore, three different kinetic mechanisms were compared in a scenario with and without EGR. The results showed that the more recent mechanisms from Konnov-2019 and NUIG Mech1.1 show similar trends in flame speeds in both scenarios. In comparison the older mechanism of Kéromnès from 2013 predicts higher flame speeds especially in the EGR case.

When more exhaust gas is recirculated and less heat is removed from the exhaust gas a second local maximum at an air factor of $\lambda = 1.0$ is obtained. This creates a plateau like maximum in flame speed in the range of $\lambda = 0.7$ and $\lambda = 1.0$. In this region, the values of flame speed are dominated equally strong by the change of diffusivity and chemical time scale with respect to air factor. For high EGR rates in the range of 1.0 and less heat loss of the EGR the maximum in flame speed is obtained for air factors of $\lambda = 1.0$.

Acknowledgements

The authors would like to acknowledge the financial support by the Friedrich and Elisabeth Boysen Foundation in the project “Premixed hydrogen combustion at high recirculation rates” (BOY-178). The present work contributes to the research on this topic.

References

[1] Andreas Dreizler, Heinz Pitsch, Christof Schulz, Johannes Janicka, Energiewende: verlässlich, machbar, technologieoffen, 2020.

[2] S. Sharma, S.K. Ghoshal, Hydrogen the future transportation fuel: From production to applications, Renewable and Sustainable Energy Reviews 43 (2015) 1151–1158.

[3] A.M. Garcia, S. Le Bras, W. Polifke, Effect of hydrogen addition on the consumption speed of lean premixed laminar methane flames exposed to combined strain and heat loss, Combust. Theory Model. (2023) 1–21.

[4] W. Zhang, J. Wang, W. Lin, R. Mao, H. Xia, M. Zhang, Z. Huang, Effect of differential diffusion on turbulent lean premixed hydrogen enriched flames through structure analysis, International Journal of Hydrogen Energy 45 (2020) 10920–10931.

[5] J. Pareja, H.J. Burbano, Y. Ogami, Measurements of the laminar burning velocity of hydrogen–air premixed flames, International Journal of Hydrogen Energy 35 (2010) 1812–1818.

[6] G.I. Sivashinsky, Instabilities, Pattern Formation, and Turbulence in Flames, Annu. Rev. Fluid Mech. 15 (1983) 179–199.

[7] H.L. Yip, A. Srna, A.C.Y. Yuen, S. Kook, R.A. Taylor, G.H. Yeoh, P.R. Medwell, Q.N. Chan, A Review of Hydrogen Direct Injection for Internal Combustion Engines: Towards Carbon-Free Combustion, Applied Sciences 9 (2019) 4842.

[8] F.H. Vance, L. de Goey, J.A. van Oijen, Development of a flashback correlation for burner-stabilized hydrogen-air premixed flames, 0010-2180 243 (2022) 112045.
[9] M.T. Chaichan, Characterization of Lean Misfire Limits of Mixture Alternative Gaseous Fuels Used for Spark Ignition Engines, Tikrit Journal of Engineering Sciences 19 (2012) 50–61.
[10] M.T. Chaichan, Practical study of compression ratio, spark timing and equivalence ratio effects on SIE fueled with hydrogen, Proceeding to Industrial Applications of Energy Systems, Sohar University, Oman (2008).
[11] P. Chiesa, G. Lozza, L. Mazzocchi, in: Proceedings of the ASME Turbo Expo 2003: Presented at the 2003 ASME Turbo Expo, June 16 - 19, 2003, Atlanta, Georgia, American Society of Mechanical Engineers, New York, NY, 2003, pp. 163–171.
[12] C. Lu, L. Zhang, C. Cao, X. Chen, C. Xing, H. Shi, L. Liu, P. Qiu, The effects of N2 and steam dilution on NO emission for a H2/Air micromix flame, International Journal of Hydrogen Energy 47 (2022) 27266–27278.
[13] W. Shang, X. Yu, W. Shi, X. Xing, Z. Guo, Y. Du, H. Liu, S. Wang, Effect of exhaust gas recirculation and hydrogen direct injection on combustion and emission characteristics of a n-butanol SI engine, International Journal of Hydrogen Energy 45 (2020) 17961–17974.
[14] Miqdam Tariq Chaichan, EGR effects on hydrogen engines performance and emissions, International Journal fo Scientific & Engineering Research 6 (2016) 80–90.
[15] M. Ditaranto, T. Heggset, D. Berstad, Concept of hydrogen fired gas turbine cycle with exhaust gas recirculation: Assessment of process performance, Energy 192 (2020) 116646.
[16] S. Verhelst, J. Vancoillie, K. Naganuma, M. de Paepe, J. Dierickx, Y. Huyghebaert, T. Wallner, Setting a best practice for determining the EGR rate in hydrogen internal combustion engines, International Journal of Hydrogen Energy 38 (2013) 2490–2503.
[17] D. Thomas Koch, A. Sousa, D. Bertram, in: SAE Technical Paper Series, SAE International400 Commonwealth Drive, Warrendale, PA, United States, 2019.
[18] A.M. Nande, S. Szwaja, J. Naber, Impact of EGR on combustion processes in a hydrogen fuelled SI engine, 2008.
[19] B.C. Duva, E. Toulson, Unstretched unburned flame speed and burned gas Markstein length of diluted hydrogen/air mixtures, International Journal of Hydrogen Energy 47 (2022) 9030–9044.
[20] S. Wang, Y. Zhai, Z. Wang, R. Hou, T. Zhang, C. Ji, Comparison of air and EGR with different water fractions dilutions on the combustion of hydrogen-air mixtures, Fuel 324 (2022) 124686.
[21] ANSYS, Inc., ANSYS Chemkin-Pro Reaction Workbench User's Manual, Canonsburg, 2021.
[22] R J Kee, J F Grcar, M D Smooke, J A Miller, E Meeks, PREMIX: a fortran program for modeling steady laminar one-dimensional premixed flames, 1985.
[23] A.A. Konnov, Yet another kinetic mechanism for hydrogen combustion, Combustion and Flame 203 (2019) 14–22.
[24] Y. Wu, S. Panigrahy, A.B. Sahu, C. Bariki, J. Beeckmann, J. Liang, A.A. Mohamed, S. Dong, C. Tang, H. Pitsch, Z. Huang, H.J. Curran, Understanding the antagonistic effect of methanol as a component in surrogate fuel models: A case study of methanol/n-heptane mixtures, 0010-2180 226 (2021) 229–242.
[25] A. Kéromnès, W.K. Metcalfe, K.A. Heufer, N. Donohoe, A.K. Das, C.-J. Sung, J. Herzler, C. Naumann, P. Griebel, O. Mathieu, M.C. Krejci, E.L. Petersen, W.J. Pitz, H.J. Curran, An experimental and detailed chemical kinetic modeling study of hydrogen and syngas mixture oxidation at elevated pressures, Combust. Flame 160 (2013) 995–1011.
[26] C. Olm, I.G. Zsély, R. Pálvölgyi, T. Varga, T. Nagy, H.J. Curran, T. Turányi, Comparison of the performance of several recent hydrogen combustion mechanisms, 0010-2180 161 (2014) 2219–2234.
[27] L. Selle, T. Poinsot, B. Ferret, Experimental and numerical study of the accuracy of flame-speed measurements for methane/air combustion in a slot burner, 0010-2180 158 (2011) 146–154.